Improved V² Constant On-Time Control with State-Trajectory Control

Virginia Li, Qiang Li, Fred C. Lee Center for Power Electronics Systems Virginia Polytechnic Institute and State University Blacksburg, VA 24061 USA liv@vt.edu, lqvt@vt.edu, fclee@vt.edu

Abstract—Voltage regulator for smartphone microprocessor applications, such as CPU and GPU, need to meet stringent load transient requirements. A popular variable-frequency control for voltage regulator application is the Constant On-Time (COT) control due to its high light-load efficiency and high bandwidth design to achieve fast transient. In addition, the V² COT control naturally has a very high bandwidth to achieve fast transient response. However, during fast load transient demands of the microprocessors, it is possible for V2 COT control to lose control for a period of time. As a result, the output voltage of the voltage regulator will not only have a large undershoot but also a ringback, which significantly increases settling time before control is regained. The best transient response is a single-cycle response, which can be achieved using time-optimal and near time-optimal control methods. Prior arts to realize time-optimal and near time-optimal control involve complicated algorithm which need to be digitally calculated and implemented. In this paper, an analog method to achieve a single-cycle response by improving V2 COT control using state-trajectory control is proposed.

Keywords—Voltage regulator, smartphone VRM, Constant On-Time (COT) control, transient, state-plane trajectory control

I. INTRODUCTION

The arrival of 5G network and system on chip (SoC) has allowed smartphone to integrate more desktop functionalities as well as faster and more customer satisfactory streaming, gaming, and virtual reality capabilities. The increase in CPU and GPU intensive functions of the smartphone has also increased the demand of performance from the power management ICs (PMICs). Current PMIC designs comprise of an upward of 20 voltage regulators (VRs) for the various functions of the smartphone. Specifically, the VRs providing power to the CPU and GPU are required to supply high load current (i₀) while meeting the stringent output voltage (v_o) regulation requirements. To meet these requirements, bulky and costly output capacitors are necessary as energy storing units. As a result, the capacitors occupy a large amount of the board footprint, preventing a compact design.

To reduce the amount of capacitors, the VRs need to utilize

control methods with high-bandwidth designs. A popular variable-frequency current-mode control which can achieve high-bandwidth design is the Constant On-Time control (COT) and its V^2 variation [1]-[10]. The nature of the COT control is having a fixed on-time (T_{on}). With the various operating points of the system, the operation switching frequency (f_{sw}) will vary due to the fixed T_{on} . However, during a fast and/or heavy load step-up transient, the transient response of the COT control is limited by the fixed T_{on} and a predetermined $T_{off_{min}}$. The limitation of the transient response speed can result in unacceptable v_o undershoot and overshoot.

The best transient response, a single-cycle response, can be achieved using a transient-only control: the Time-Optimal Control (TOC) [11], [12]. By calculating the optimal T_{on} value under any transient condition using time-domain information, the system settles into steady-state in one switching-cycle after a transient occurs. This method not only minimizes the v_o undershoot during a load step-up transient, but also minimizes the settling time. However, the realization of TOC requires a complicated algorithm, accurate sensing of all the converter parameters, and delay-free processing of the algorithm in real-time. Aside from the realization of the TOC algorithm, additional transition algorithms are necessary as the system switches between the steady-state and transient controls.

For ease of realization, methods known as Near Time-Optimal Control (NTOC) simplify the TOC algorithm and reduce the amount of converter parameters to achieve a near-optimal transient response [13]-[17]. After a load step-up transient occurs, NTOC provide a Ton extension such that the system will reach the vicinity of the desired steady-state and rely on the steady-state control to bring the system into steady-state. By doing so, the transient response is similar to TOC while the implementation can be greatly simplified. However, NTOC algorithm still needs additional transition algorithms as the system switches between the steady-state and transient controls. Since NTOC relies on steady-state control to bring the system back into steady-state, the performance of the transition algorithm is critical to the performance of the transient response.

Near-optimal transient response without the need of transition algorithms can be achieved using the state-plane

This work is supported by the National Science Foundation under award no. 1653156.

trajectory control [18]. The state-plane trajectory control is also a transient-only control but uses state-plane information instead of time-domain information. In the state-plane, the transient behavior of the system is more clearly visualized. By calculating the optimal switching-point between the on and off state-plane trajectories, the system settles into the vicinity of the steady-state in one switching-cycle after a transient occurs. In this method, the steady-state control is the COT control with adaptive voltage positioning (AVP) and the transient control is the state-plane trajectory control. By disabling and enabling the turn-off mechanism of the COT control on-time generator, the system is able to seamlessly transition between the steady-state and transient controls. However, the stateplane trajectory control used in this method relies on the information provided by the AVP load-line, which does not exist for PMIC applications. As such, a state-plane trajectory control which does not depend on AVP load-line information is necessary.

In this paper, a state-plane trajectory control with nearoptimal transient response is proposed for PMIC applications. Unlike the prior methods, the steady-state control of the proposed method is the V² COT control, a more advanced COT control, and the transient control is the state-plane trajectory control which relies on the derivative of vo and io. The proposed method uses the control signals of the V² COT to detect the beginning and the end of the load step-up transient. When the beginning of the load step-up transient is detected, the turn-off mechanism of the Ton generator is disabled. At this instance, V2 COT control transitions seamlessly into the state-trajectory control to extend Ton. While in state-trajectory control, the converter will follow its natural on state-trajectory until the optimal-switching point to achieve the fastest transient response possible. After the end of the load step-up transient is detected, the control transitions seamlessly back into V² COT control by enabling the turn-off mechanism of the Ton generator.

To better understand the proposed method, the state-plane trajectory analysis of a buck converter is presented in Section II. The state-plane representation of a V² COT-controlled buck converter and the proposed state-plane representation of its control law are presented in Section III. The proposed state-trajectory control with single-cycle response is presented in Section IV. Finally, the simulation and hardware verification of the proposed method are presented in Section V.

II. STATE-PLANE TRAJECTORY OF BUCK CONVERTER

The power stage of the VR is typically a synchronous buck converter, composed of an input source voltage (V_{in}) , MOSFET switches S_1 and S_2 , inductor (L), output capacitor (C_o) with parasitic resistance (R_{co}) , and load current (i_o) , as shown in Fig. 1. In continuous conduction mode (CCM), the operation of the buck converter is a piece-wise function of its two stages: on-stage, with S_1 closed and S_2 open, and off-stage, with S_1 open and S_2 closed.

Each stage of the buck converter is a linear system which can be represented using a state-space model. By defining the state variables as the energy storing elements, capacitor voltage (v_{co}) and inductor current (i_L) , the behavior of the energy in the system can be clearly described using the state-space model, as given in TABLE I.

To understand the behavior of the state variables, first, the state-variable solutions need to be obtained by solving the state-space models. Then, assuming the buck converter operates in each stage for a short period of time such that $t-t_0 < \pi \sqrt{LC_o}$, the state-variable solutions can be simplified as (1) and (2), where $v_{co}(t_0)$ and $i_L(t_0)$ are the initial conditions of each stage, the resonant frequency (ω_0) is given by (3), characteristic impedance (Z_0) is given by (4), and equilibrium voltage (V_E) and equilibrium current (I_E) are given in TABLE I. To further simplify, the solutions can be mapped to the state-plane as state-plane trajectories.

The axes of the state-plane are defined by the normalized state variables, $v_{\rm coN}$ and $i_{\rm LN}$; the state variables are normalized by multiplying voltages by the normalizing factor $V_{\rm N}$, given by (5), and currents by the normalizing factor $I_{\rm N}$, given by (6). Duration of time in the state-plane is represented as an angle (θ), given by (7). As such, the normalized solutions for each stage are given by (8) and (9), where $V_{\rm co0N}$ and $I_{\rm L0N}$ are the normalized initial conditions of the stage. Combining (8) and (9), the normalized state-plane trajectory for each stage is given in TABLE II and drawn in the state-plane in Fig. 2.

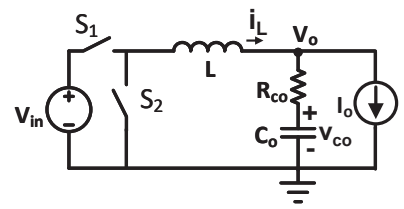


Fig. 1. Synchronous buck converter topology.

TABLE I. STATE-SPACE MODELS OF THE BUCK CONVERTER IN CCM

Converter Stage	State-Space Model	$\mathbf{V}_{_{E}}$	I
On-stage	$ \begin{bmatrix} \dot{v_{co}} \\ \dot{i_L} \end{bmatrix} = \begin{bmatrix} 0 & \frac{1}{C_o} \\ -\frac{1}{L} & -\frac{R_{co}}{L} \end{bmatrix} \begin{bmatrix} v_{co} \\ \dot{i_L} \end{bmatrix} + \begin{bmatrix} 0 \\ \frac{1}{L} \end{bmatrix} V_{in} + \begin{bmatrix} -\frac{1}{C_o} \\ \frac{R_{co}}{L} \end{bmatrix} I_o $	V	I
Off-stage	$ \begin{bmatrix} v_{co} \\ i_L \end{bmatrix} = \begin{bmatrix} 0 & \frac{1}{c_o} \\ -\frac{1}{L} & -\frac{R_{co}}{L} \end{bmatrix} \begin{bmatrix} v_{co} \\ i_L \end{bmatrix} + \begin{bmatrix} -\frac{1}{c_o} \\ \frac{R_{co}}{L} \end{bmatrix} I_o $	0	I

$$v_{co}(t) \approx V_E + [v_{co}(t_0) - V_E] \cos(\omega_0 t) + [(i_L(t_0) - I_E)Z_0] \sin(\omega_0 t)$$
 (1)

$$i_{L}(t) \approx I_{E} + [i_{L}(t_{0}) - I_{E}] \cos(\omega_{0}t) - [(v_{co}(t_{0}) - V_{E}) \frac{1}{Z_{0}}] \sin(\omega_{0}t)$$
 (2)

In the normalized state-plane, the behavior of the state variables can be clearly observed. For each converter stage, the normalized state-plane trajectory is a circle traveling in the counterclockwise direction from the initial conditions, representing the resonance and transfer of energy in the between the inductor and capacitor. The centers of the trajectory circles are given by the normalized equilibrium points, V_{EN} and I_{EN} , representing the operating point of each stage. The radii of the circles, ρ_{ON} and ρ_{OFF} , are given by the centers and the initial conditions of each stage, representing the amount of energy circulating in the system. By examining the state-trajectory of the buck converter in the state-plane, it will provide a better insight into the behavior of the system not only in steady-state, but also during transient.

III. Proposed State-Plane Representation of $V^2\ COT$ Control Law

A. Steady-state of V² COT Control

The general circuit representation of a buck converter with V^2 COT control is shown in Fig. 3 and its steady-state operation is shown in Fig. 4. As previously mentioned, the operation of the buck converter is a piece-wise function of its on- and off-stages. The duty cycle (D) of the converter is the ratio of V_o to V_{in} . The amount of time the converter is operating in the on- and off-stages correspond to T_{on} and T_{off} respectively. To ensure v_o is operating at the desired voltage set by the CPU, v_o is compared with a reference voltage (V_{ref}).

$$\omega_0 = \frac{1}{\sqrt{LC_o}} \tag{3}$$

$$Z_0 = \sqrt{\frac{L}{C_o}} \tag{4}$$

$$I_N = \frac{Z_0}{V_{in}} \tag{5}$$

$$V_N = \frac{1}{V_{in}} \tag{6}$$

$$\theta = \omega_0(t - t_0) \tag{7}$$

$$v_{coN} - V_{EN} = (V_{o0N} - V_{EN})cos\theta + (I_{L0N} - I_{EN})sin\theta$$
 (8)

$$i_{LN} - I_{EN} = (I_{L0N} - I_{EN})\cos\theta - (V_{o0N} - V_{EN})\sin\theta$$
 (9)

TABLE II. NORMALIZED STATE-PLANE TRAJECTORY OF THE BUCK CONVERTER

Converter Stage	Normalized State-Plane Trajectory Equation	V _{EN}	I EN
On-stage	$\begin{split} \rho_{ON} &= \sqrt{(\nu_{coN} - 1)^2 + (i_{LN} - I_{oN})^2} \\ &= \sqrt{(V_{co0N} - 1)^2 + (I_{L0N} - I_{oN})^2} \end{split}$	1	I
Off-stage	$\rho_{OFF} = \sqrt{(v_{coN})^2 + (i_{LN} - I_{oN})^2}$ $= \sqrt{(v_{coN})^2 + (I_{LON} - I_{oN})^2}$	0	I

The V^2 COT control law, given by (10), is the instance v_o falls and intersects with V_{ref} to determine the beginning of T_{on} . Afterwards, a fixed T_{on} is given. One implementation to realize fixed T_{on} is by comparing a fixed ramp signal (S_r) to a fixed threshold voltage (V_{th}). The end of T_{on} is determined when S_r rises and intersects with V_{th} . As shown in Fig. 4, V^2 COT operates in the region where $V_{ref} < v_o$.

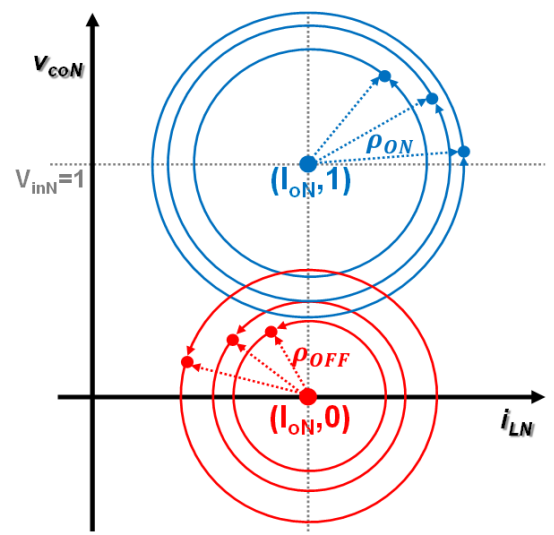


Fig. 2. The normalized state-trajectory of the buck converter during on-stage (blue) and off-stage (red).

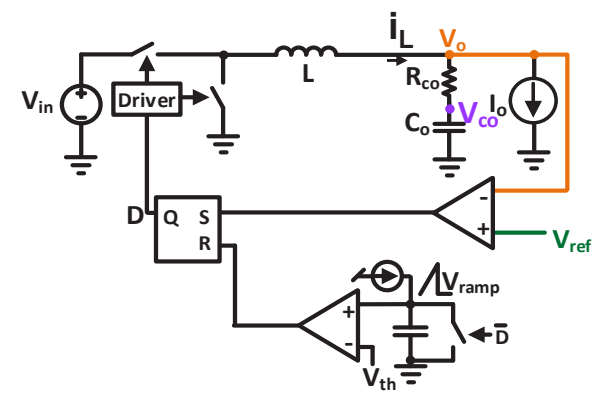


Fig. 3. General control scheme of a buck converter with V2 COT control.

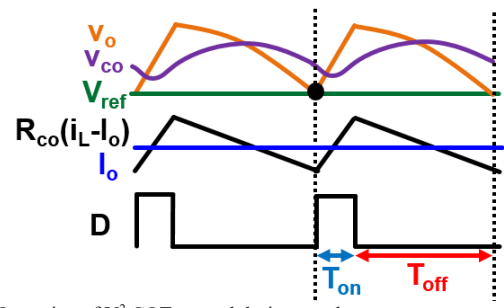


Fig. 4. Operation of V² COT control during steady-state.

The state-plane trajectory of the buck converter with V² COT control in steady-state is shown in Fig. 5. For a given V_{ref} and I_o, the control law can be drawn on the state plane as a linear line with slope of -R_{co}. The beginning of T_{on}, which lies on the COT control law in the state-plane, corresponds to the initial conditions of the on-stage trajectory. Using the initial conditions and the center of the trajectory circle, the normalized state-plane trajectory circle for the on-stage can be projected. The state-plane trajectory of the converter will follow the circular path for a fixed θ_{on} , given by (11). At the end of θ_{on} , the converter switch from the on-stage to the offstage, ending Ton. The end of Ton corresponds to the initial condition of the off-stage trajectory. Similar to the on-stage, the normalized state-plane trajectory circle for the off-stage can be projected. The state-plane trajectory of the converter will follow the circular path until it intersects the V2 COT control law and switch the converter to the on-stage. As such, the state-plane trajectory representation of the V2 COT controlled buck converter in steady-state is the piece-wised closed-loop between the on- and off-stage trajectory arcs.

$$V_{ref} = v_o = v_{co} + R_{co}(i_L - I_o)$$
 (10)

$$\theta_{on} = T_{on}\omega_0 \tag{11}$$

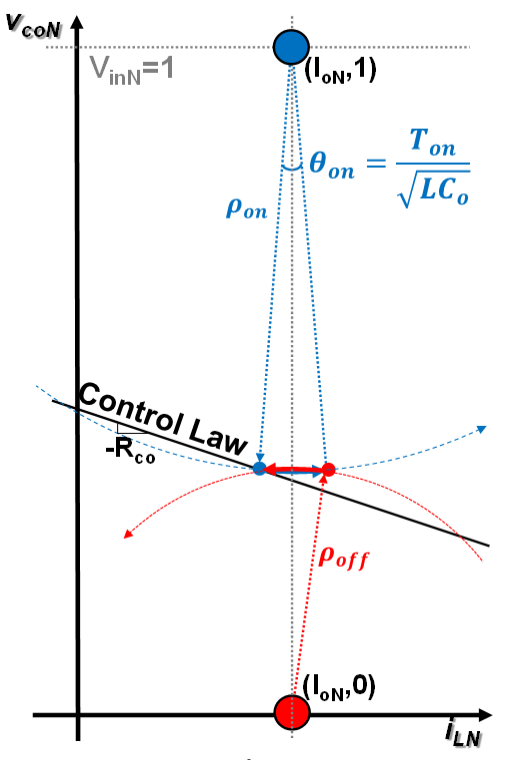


Fig. 5. State-plane representation of V^2 COT controlled buck converter during steady-state where the on-stage trajectory (blue solid) travels on the projected on-stage trajectory (blue dash) until the end of θ_{on} , where the converter switches to the off-trajectory (red solid) and travels on the projected off-trajectory trajectory (red dash) until it intersects with the control law.

B. Load Step-Up Transient of V² COT Control

A buck converter, with parameters of $V_{\rm in}$ =2.6V, $V_{\rm o}$ =0.85V, $f_{\rm sw}$ =5MHz, L=90nH, $C_{\rm o}$ =44uF, $R_{\rm co}$ =4.5m Ω and $\Delta i_{\rm o}$ =0.65-5A, is simulated in SIMPLIS to demonstrate the behavior of a buck converter with V² COT control during load step-up transient. For fast and/or heavy load changes as shown in Fig. 6, V² COT control is lost when $v_{\rm o}$ operates below $V_{\rm ref}$, between $t_{\rm o}$ and $t_{\rm A}$. During this time period, $T_{\rm on}$ is followed by a fixed minimum off-time ($T_{\rm off_min}$) before another $T_{\rm on}$ occurs. The control operates with multiple cycles of $T_{\rm on}$ and $T_{\rm off_min}$ before $v_{\rm o}$ recovers above $V_{\rm ref}$ at $t_{\rm A}$. Afterwards, control is regained when the control law condition is met at $t_{\rm B}$. Between $t_{\rm A}$ and $t_{\rm B}$, $v_{\rm o}$ can recover above the steady-state ripple, resulting in a ringback. This behavior is undesirable as it increases settling time and voltage ripple in $v_{\rm o}$.

The state-plane representation of the load step-up transient is shown in Fig. 7. When a load step transient occurs at t₀, the control law, on- and off- stage trajectory circle centers move due to the change in Io. The state-plane trajectory will follow the on-stage circle for the θ_{on} until t_1 . Then, the converter will switch to the off-stage. The trajectory will follow the off-stage circle for a fixed angle, θ_{off} , equal to $T_{off min}$. Afterwards, another on-stage trajectory occurs. Multiple cycles of the piece-wised on- and off- stage trajectories occur until the trajectory crosses above the control law at tA. After the trajectory finishes the fixed θ_{on} , the off-stage trajectory intersects the control law at t_B. Between t_A and t_B, v_{coN} operates higher than the normal steady-state values, representing the ringback which occurs in vo. The multi-cycle transient response of the V² COT control not only result in a large undershoot, settling time, but also the undesirable ringback.

IV. PROPOSED STATE-TRAJECTORY CONTROL

The fastest achievable transient is a single-cycle response. When a load step-up transient occurs and V² COT control is lost, a single-cycle response can be achieved by following the natural state-plane trajectory of the on-stage to

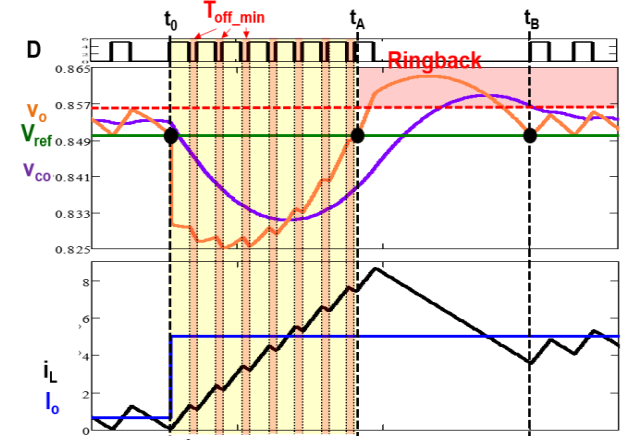


Fig. 6. Operation of V² COT control during transient.

an optimal switching point. By switching to the off-stage at this point, the off trajectory will bring the system the new steady-state in one switching cycle. The time domain waveforms of a single-cycle response are shown in Fig. 8, and its state-plane trajectory is shown in Fig. 9. As given in TABLE II, the normalized state-plane trajectory of the on- and off-stages are circles. As such, the optimal switching point $(t_{\rm E})$ can be calculated as the intersection of two circles.

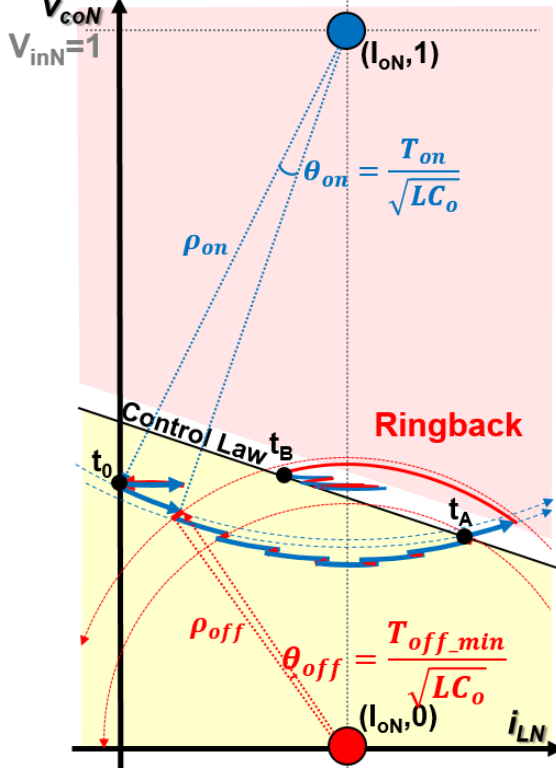


Fig. 7. State-plane representation of V^2 COT controlled buck converter during transient where multiple cycles of on-stage (blue) and off-stage (red) trajectories are required to reach the new steady-state.

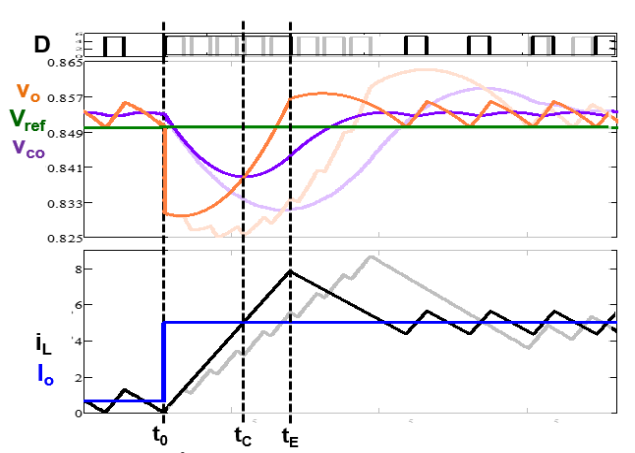


Fig. 8. Operation of V² COT with single-cycle transient response during load step-up transient.

In order to calculate t_E , trajectory circle centers and radii information are needed. The centers of both stage are given in TABLE II, and are dependent on I_{oN} . After a load transient occurs, the new I_{oN} need to be obtained. At t_c , $i_{LN} = I_{oN}$, $v_{co} = v_o$, and $dv_{coN} = 0$. By observing $dv_{coN} = 0$, I_{oN} information can be obtained by sensing i_{LN} at t_c . On the $i_{LN} = I_{oN}$ axis, the radii can be simplified to only require voltage information. As such, ρ_{on} is given by (12) and ρ_{off} is given by (13). Knowing centers and radii information, t_E can be calculated as an i_{LN} limit function, I_{xN} , given by (14), as shown in Fig. 10. However, it is not easy to implement division and square root functions using analog circuitry.

Using curve fitting method, (14) can be un-normalized and simplified to (15), which can be easily implemented using analog components. The implementation of the proposed control is shown in Fig. 11 and its operation in Fig. 12. The proposed method obtain t_c by observing $dv_{coN}=0$. However, direct access to v_{co} is not available. V_o contains v_{co} information as shown in (10). Thus, the derivative of v_o (dv_o), which contains dv_{co} information, can be used to obtain t_c . At t_c , the criteria in (16) is met.

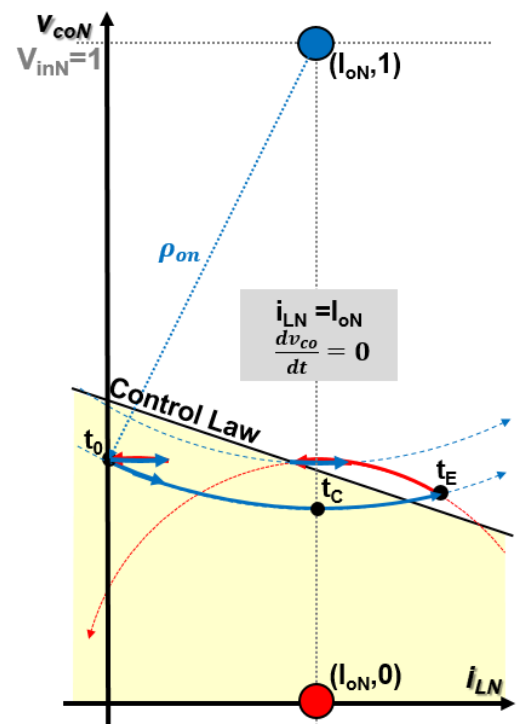


Fig. 9. The state-plane trajectory of V² COT with single-cycle response as the piece-wised function of the on-stage trajectory (blue) and the off-stage trajectory (red).

$$\rho_{on} = 1 - v_{oN} \tag{12}$$

$$\rho_{off} \approx V_{refN} \tag{13}$$

$$I_{xN} = I_{oN} + \sqrt{\frac{\rho_{on}^2 + \rho_{off}^2 - 1}{2}}$$
 (14)

$$I_x = I_o + \frac{\sqrt{2}R_{co}}{Z_0^2}V_{ref} - \sqrt{2}\frac{R_{co}}{Z_0}V_{in} + \sqrt{2}$$
 (15)

$$\frac{dv_o}{dt} = R_{co}\frac{di_L}{dt} = R_{co}\frac{V_{in} - v_o}{L} \tag{16}$$

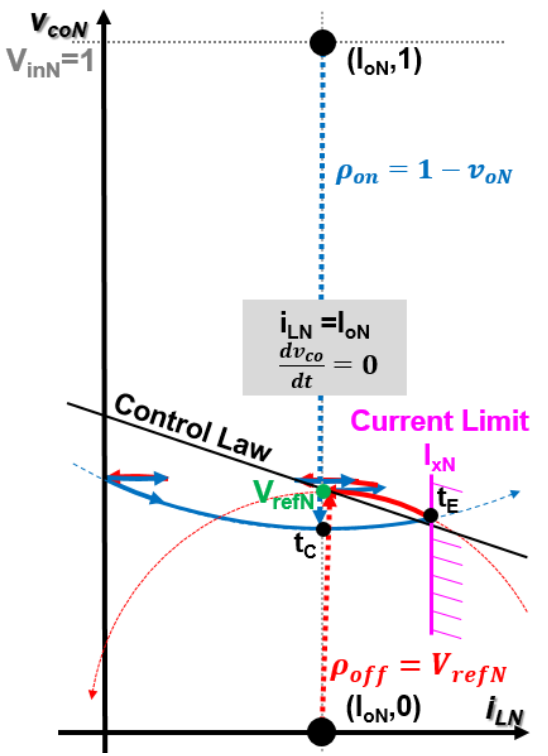


Fig. 10. The state-plane trajectory of COT with proposed state-trajectory control during load step-up transient.

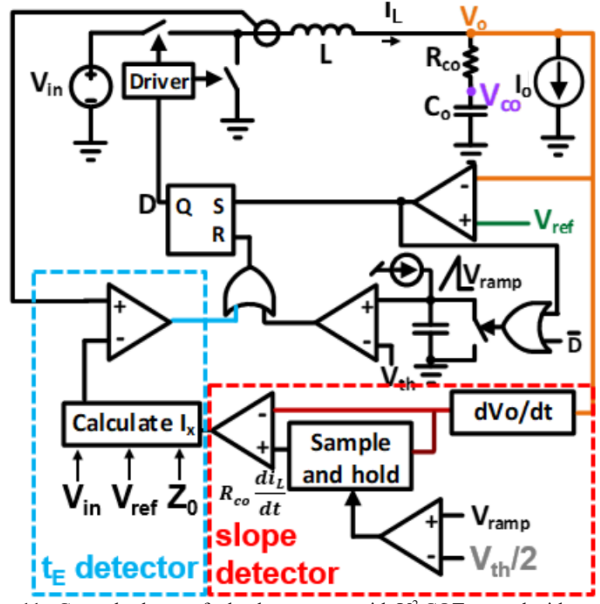


Fig. 11. Control scheme of a buck converter with V^2 COT control with state-trajectory control.

V. SIMULATION AND EXPERIMENTAL RESULTS

The worst case performance of V² COT for smartphone CPU/GPU VR application is simulated using Simplis with parameters of $V_{in}=2.6V$, $V_o=0.85V$, $f_{sw}=5MHz$, L=90nH, C_o =44uF, R_{co} =4.5m Ω , $T_{off\ min}$ =25ns, and Δi_o =0.25-5A. The transient performance of the conventional V2 COT with Toff min is compared to the proposed state-trajectory control (STC) in Fig. 13. From Fig. 13, V² COT with the proposed STC has minimized undershoot, settling time, and no ringback issue during load step-up transient. In addition, the proposed STC also reduces the inductor current stress during load step-up transient. Component tolerance effect is also studied due to its impact on the performance of the converter. A +/- 20% tolerance is considered for the L and C values. The worst case transient performance occurs when L is large and C is smallest. The worst case transient performance with component tolerance effect of the conventional V2 COT and with the proposed STC is shown in Fig. 14. From Fig. 14, the proposed STC is still able to achieve the best transient response without any ringback issues.

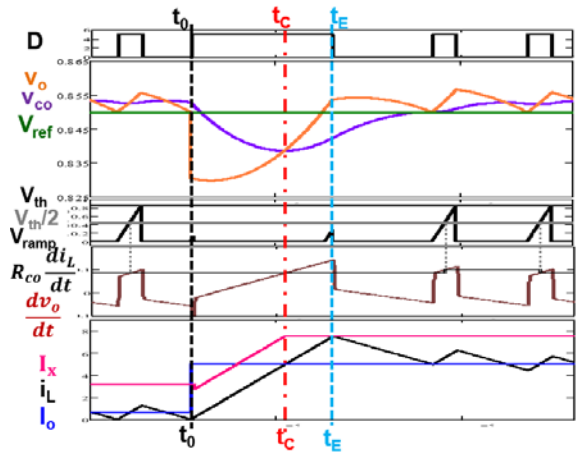


Fig. 12. Operation of proposed state-trajectory control.

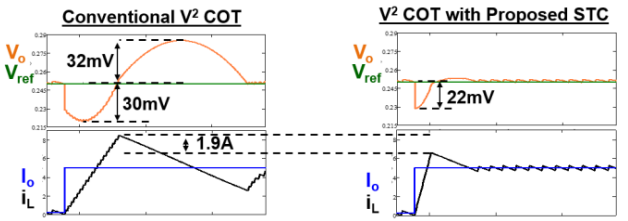


Fig. 13. Time-domain worst-case transient performance of conventional V^2 COT with $T_{\rm off\ min}$ vs. proposed state-trajectory control.

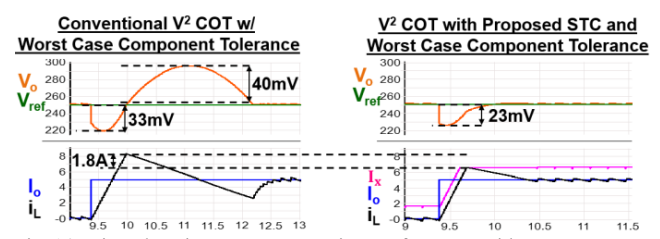


Fig. 14. Time-domain worst-case transient performance with component tolerance of conventional V^2 COT with T_{off_min} vs. proposed state-trajectory control.

IC delay effect is also considered in addition to the component tolerance effect due to the high operating frequency of the converter. A 10ns delay per comparator is considered. The worst case transient performance with component tolerance and IC delay effects of the conventional V^2 COT and with the proposed STC is shown in Fig. 15. From Fig. 13 to Fig. 15, it can be observed the proposed STC is able to minimize $v_{\rm o}$ settling time, undershoot, ringback, and $i_{\rm L}$ stress compared to conventional V^2 COT under typical operation tolerances.

A control card with V^2 COT and the proposed state-plane trajectory control is built using discrete components and connected to a buck power-stage to obtain the experimental results. Due the use of discrete components for the control card, noise can significantly interfere with the operation of the control, making it difficult to operate at the high switching frequency of 5MHz. Instead, the control will operate at 300kHz to prove the concept of the proposed method. To achieve high frequency operation, it is necessary to fabricate the control using integrated chip (IC) designs.

For a single-phase operation with V_{in} =5V, V_{ref} =1.2V, f_{sw} =300kHz, and I_o =0-4A, the time-domain load step-up transient performance of V² COT is shown in Fig. 16 and V² COT with the proposed state-plane trajectory control is shown in Fig. 17. With the proposed state-plane trajectory control, the undershoot is minimized, the 10mV overshoot of V² COT is eliminated, and the V_o settling time is minimized from 8.5us to 3.5us. A zoomed-in, more detailed operation of the proposed control waveforms are shown in Fig. 18.

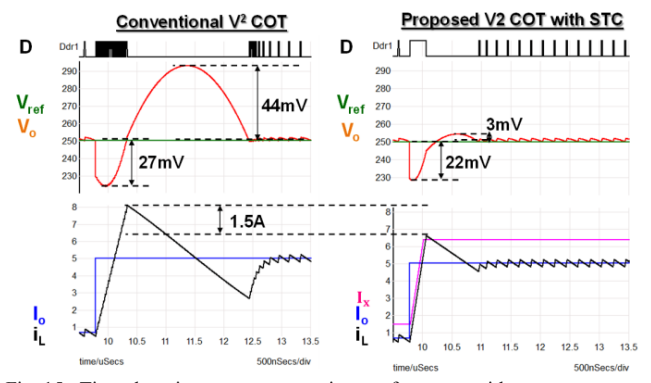


Fig. 15. Time-domain worst-case transient performance with component tolerance and IC delay effects of conventional V^2 COT with $T_{\text{off_min}}$ vs. proposed state-trajectory control.

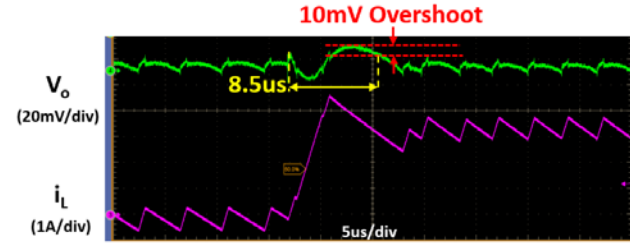


Fig. 16. V²COT during load step-up transient.

VI. CONCLUSION

In this paper, an improved V² COT control with state-plane trajectory control to achieve near-optimal transient response is proposed for PMIC applications. The state-plane trajectory control is a transient-only control which can achieve the best transient response possible, a single-cycle response. The proposed state-plane trajectory control utilizes io and V_{ref} information to estimate the vicinity of the new steady-state. An implementation which obtain io by monitoring the derivative of vo and sampling iL at a given condition is presented. Using information used to estimate the new steadystate, the optimal switching point can be determined as the intersection of the on- and off-trajectory circles and realized as a current limiting wall function. From the simulation and experimental results presented, the proposed method is able to minimize vo undershoot, settling time, and eliminate ringback issue associated with the V² COT control transient response. So for a given v₀ ripple undershoot, the proposed control has the ability to use less output capacitor, thus reducing board footprint. Additional work is being conducted to further simplify the state-plane trajectory control through implementation with capacitor current information and multiphase operation.

ACKNOWLEDGMENT

This work is supported by the National Science Foundation under Award no. 1653156.

DISCLAIMER

Any opinions, findings, conclusions, or recommendations expressed in this paper are those of the author(s) and do not reflect the views of the National Science Foundation.

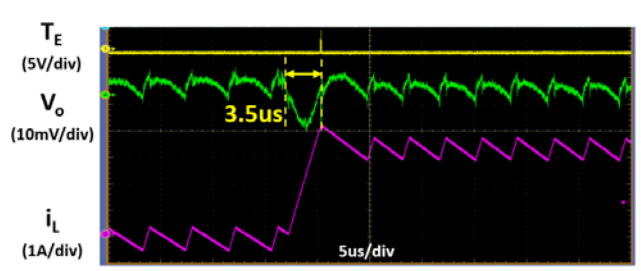


Fig. 17. V²COT with proposed state-plane trajectory control during load step-up transient.

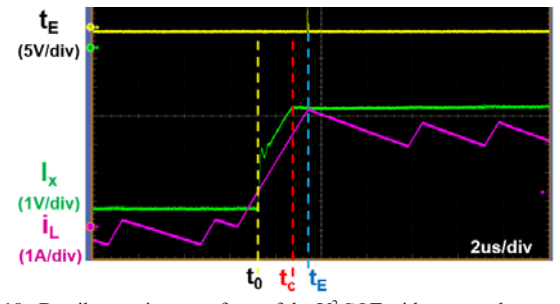


Fig. 18. Detail operation waveform of the V²COT with proposed state-plane trajectory control during load step-up transient.

REFERENCES

- [1] Y. Yan, F. C. Lee and P. Mattavelli, "Comparison of Small Signal Characteristics in Current Mode Control Schemes for Point-of-Load Buck Converter Applications," in *IEEE Transactions on Power Electronics*, vol. 28, no. 7, pp. 3405-3414, July 2013.
- [2] K. Cheng, F. Yu, P. Mattavelli and F. C. Lee, "Characterization and performance comparison of digital V²-type constant on-time control for buck converters," 2010 IEEE 12th Workshop on Control and Modeling for Power Electronics (COMPEL), Boulder, CO, 2010, pp. 1-6.
- for Power Electronics (COMPEL), Boulder, CO, 2010, pp. 1-6.

 [3] F. Yu and F. C. Lee, "Design oriented model for constant on-time V2control," 2010 IEEE Energy Conversion Congress and Exposition, Atlanta, GA, 2010, pp. 3115-3122.
- [4] S. Tian, F. C. Lee, P. Mattavelli, K. Cheng and Y. Yan, "Small-Signal Analysis and Optimal Design of External Ramp for Constant On-Time V² Control With Multilayer Ceramic Caps," in *IEEE Transactions on Power Electronics*, vol. 29, no. 8, pp. 4450-4460, Aug. 2014.
- Power Electronics, vol. 29, no. 8, pp. 4450-4460, Aug. 2014.

 [5] S. Tian, F. C. Lee, Q. Li and Y. Yan, "Unified Equivalent Circuit Model and Optimal Design of V² Controlled Buck Converters," in *IEEE Transactions on Power Electronics*, vol. 31, no. 2, pp. 1734-1744, Feb. 2016.
- [6] Y. Yan, F. C. Lee, S. Tian and P. Liu, "Modeling and Design Optimization of Capacitor Current Ramp Compensated Constant On-Time V² Control," in *IEEE Transactions on Power Electronics*, vol. 33, no. 8, pp. 7288-7296, Aug. 2018.
- [7] Linear Technology. (2010). LTC3833: Fast Accurate Step-Down DC/DC Controller with Differential Output Sensing. [Online]. Available: http://cds.linear.com/docs/en/datasheet/3833f.pdf
- [8] Texas Instruments. (2012, Jan.). TPS51650/TPS59650 Dual-Channel (3-Phase CPU/2-Phase GPU) SVID, D-CAP+ Step-Down Controller for IMVP-7 V_{core} with Two Integrated Drivers. [Online]. Available: http://www.ti.com/lit/ds/symlink/tps59650.pdf
- [9] Richtek. (2016, Nov.) RT8096A 1A, 1.5MHz 6V CMCOT Synchronous Step-Down Converter. [Online]. Available: https://www.richtek.com/assets/product_file/RT8096A/DS8096A-04.pdf
- [10] R. B. Vasconselos and M. L. S. Martins, "A hybrid digital control method for synchronous buck converters using multisampled linear PID and V²constant on-time controllers," 2017 Brazilian Power Electronics Conference (COBEP), Juiz de Fora, 2017, pp. 1-6.
- [11] W.W. Burns and T. G. Wilson, "Analytic derivation and evaluation of a state-trajectory control law for DC-to-DC- converters," 1977 IEEE Power Electronics Specialists Conference, Palo Alto, CA, USA, 1977, pp.70.85.
- pp.70.85.

 D. Biel, L. Martinez, J. Tenor, B. Jammes and J. C. Marpinard, "Optimum dynamic performance of a buck converter," *Circuits and Systems*, 1996. ISCAS '96 Connecting the World., 1996 IEEE International Symposium on, Atlanta, GA, 1996, pp. 589-592 vol.1.
- [13] G. Feng, E. Meyer and Y. F. Liu, "A New Digital Control Algorithm to Achieve Optimal Dynamic Performance in DC-to-DC Converters," in *IEEE Transactions on Power Electronics*, vol. 22, no. 4, pp. 1489-1498, July 2007.
- [14] E. Meyer, Z. Zhang and Y. Liu, "An Optimal Control Method for Buck Converters Using a Practical Capacitor Charge Balance Technique," in *IEEE Transactions on Power Electronics*, vol. 23, no. 4, pp. 1802-1812, July 2008.
- [15] L. Corradini, A. Costabeber, P. Mattavelli and S. Saggini, "Time optimal, parameter insensitive digital controller for VRM applications with Adaptive Voltage Positioning," 2008 11th Workshop on Control and Modeling for Power Electronics, Zurich, 2008, pp. 1-8.
- [16] V. Yousefzadeh, A. Babazadeh, B. Ramachandran, E. Alarcon, L. Pao and D. Maksimovic, "Proximate Time-Optimal Digital Control for Synchronous Buck DC–DC Converters," in *IEEE Transactions on Power Electronics*, vol. 23, no. 4, pp. 2018-2026, July 2008.
- [17] V. I. Kumar and S. Kapat, "Unified Digital Current Mode Control Tuning With Near Optimal Recovery in a CCM Buck Converter," in *IEEE Transactions on Power Electronics*, vol. 31, no. 12, pp. 8461-8470, Dec. 2016.
- [18] V. Li, Q. Li, F. C. Lee and P. Liu, "State-Trajectory Control With Single-Cycle Response for Point-of-Load Converters," in *IEEE Transactions on Industrial Electronics*, vol. 67, no. 4, pp. 3157-3166, April 2020.